



Perovskite Oxides: Spin Transport and Dynamics

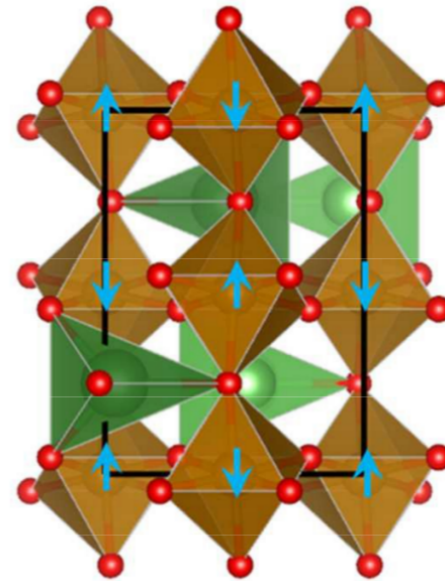
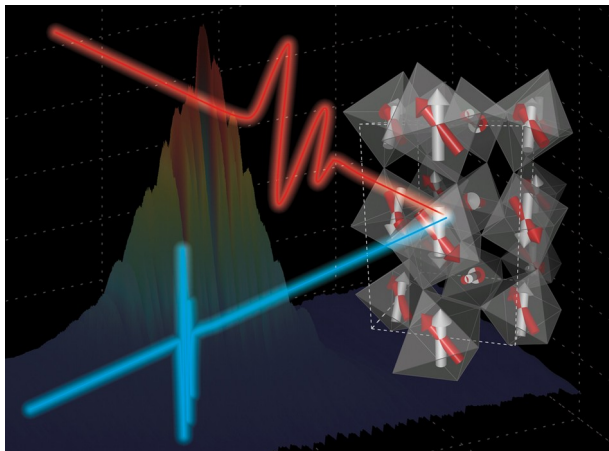
Jiwuer Jilili, Mousumi Upadhyay Kahaly

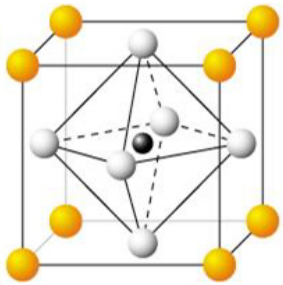
Computational and Applied Materials Science (CAMS)

2018.07.03.



- ▶ Introduction & Motivation
- ▶ Computational perspective
- ▶ $\text{LaNiO}_3/\text{CaMnO}_3$; $\text{BiMnO}_3/\text{SrTiO}_3$
- ▶ Electronic structure and spin transport
- ▶ Summary





A(yellow): rare-earth or alkali-metal cation
 B(black): transition metal cation

Manganites: $LaMnO_3$, $CaMnO_3$

Titantes: $SrTiO_3$, $LaTiO_3$, $CaTiO_3$

Ferrites: $BiFeO_3$, $LuFe_2O_4$

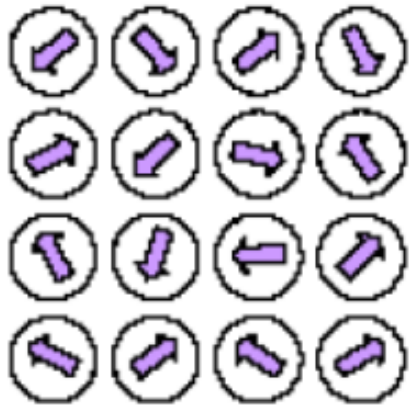
Group	1	2	3	4	5	6	7	8	9	10	11	12	13	14	15	16	17	18
Period 1	1 H																	2 He
2	3 Li	4 Be											5 B	6 C	7 N	8 O	9 F	10 Ne
3	11 Na	12 Mg											13 Al	14 Si	15 P	16 S	17 Cl	18 Ar
4	19 K	20 Ca	21 Sc	22 Ti	23 V	24 Cr	25 Mn	26 Fe	27 Co	28 Ni	29 Cu	30 Zn	31 Ga	32 Ge	33 As	34 Se	35 Br	36 Kr
5	37 Rb	38 Sr	39 Y	40 Zr	41 Nb	42 Mo	43 Tc	44 Ru	45 Rh	46 Pd	47 Ag	48 Cd	49 In	50 Sn	51 Sb	52 Te	53 I	54 Xe
6	55 Cs	56 Ba	57-71	72 Hf	73 Ta	74 W	75 Re	76 Os	77 Ir	78 Pt	79 Au	80 Hg	81 Tl	82 Pb	83 Bi	84 Po	85 At	86 Rn
7	87 Fr	88 Ra	89-103	104 Rf	105 Db	106 Sg	107 Bh	108 Hs	109 Mt	110 Ds	111 Rg	112 Cn	113 Uut	114 Fl	115 Uup	116 Lv	117 Uus	118 Uuo

57 La	58 Ce	59 Pr	60 Nd	61 Pm	62 Sm	63 Eu	64 Gd	65 Tb	66 Dy	67 Ho	68 Er	69 Tm	70 Yb	71 Lu
89 Ac	90 Th	91 Pa	92 U	93 Np	94 Pu	95 Am	96 Cm	97 Bk	98 Cf	99 Es	100 Fm	101 Md	102 No	103 Lr

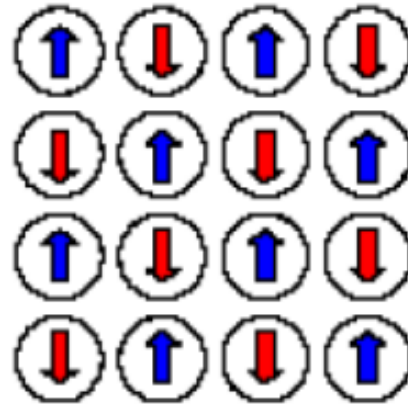
Band gap tuning: optoelectronic application; Efficient solar cells; Transparent conducting oxides.

$SrTiO_3$: 3.2 eV; $CaMnO_3$: 3.1 eV; $BiMnO_3$: 0.9 eV; $LaMnO_3$: 1.7 eV

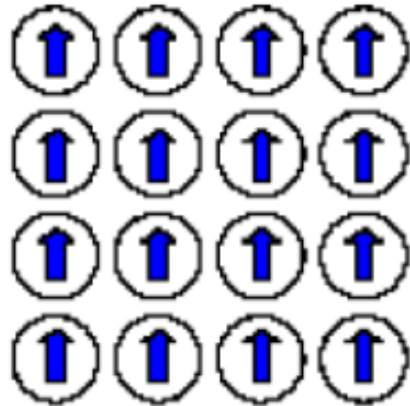
Perovskite Oxides: spin orderings



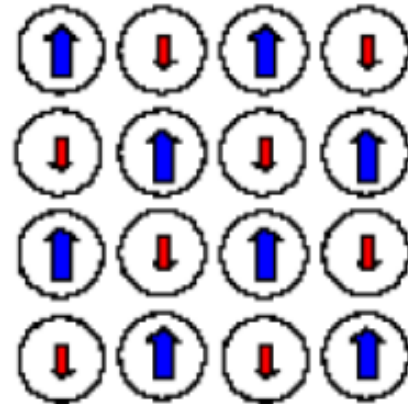
Paramagnetic



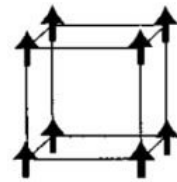
Antiferromagnetic



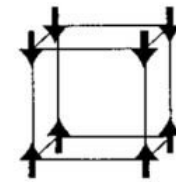
Ferromagnetic



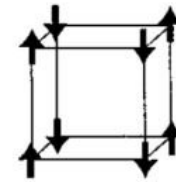
Ferrimagnetic



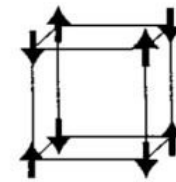
FM



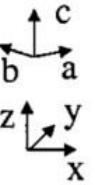
AFM(A)



AFM(C)



AFM(G)

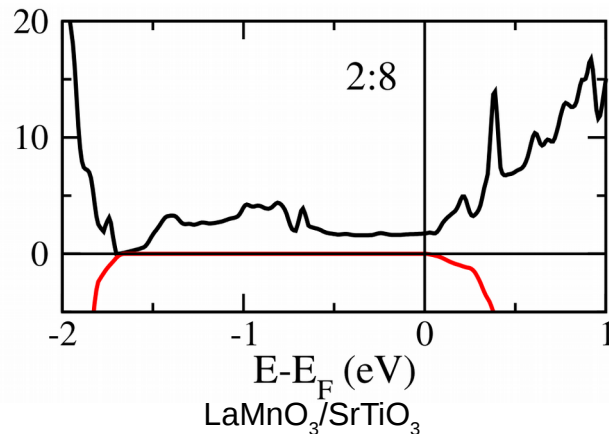


1998 review by Imada, Fujimori and Tokura (page 1122)

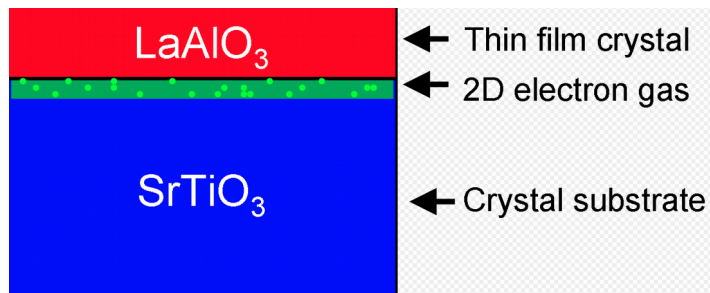
NM: SrTiO_3 , PbTiO_3 ...

FM: La(Sr)MnO_3 , BiMnO_3 , SrRuO_3

AFM: LaMnO_3 , CaMnO_3 ...



DOI: 10.1038/srep13762



<https://en.wikipedia.org/wiki/>



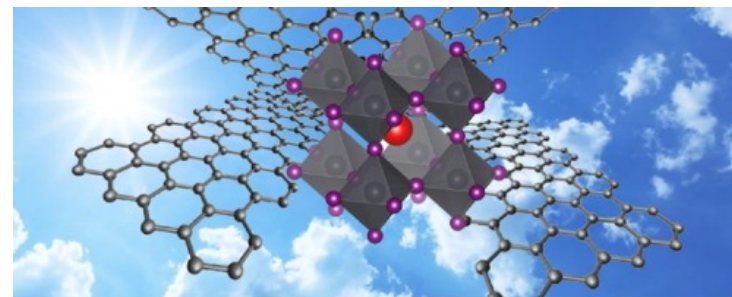
Variety of novel properties:

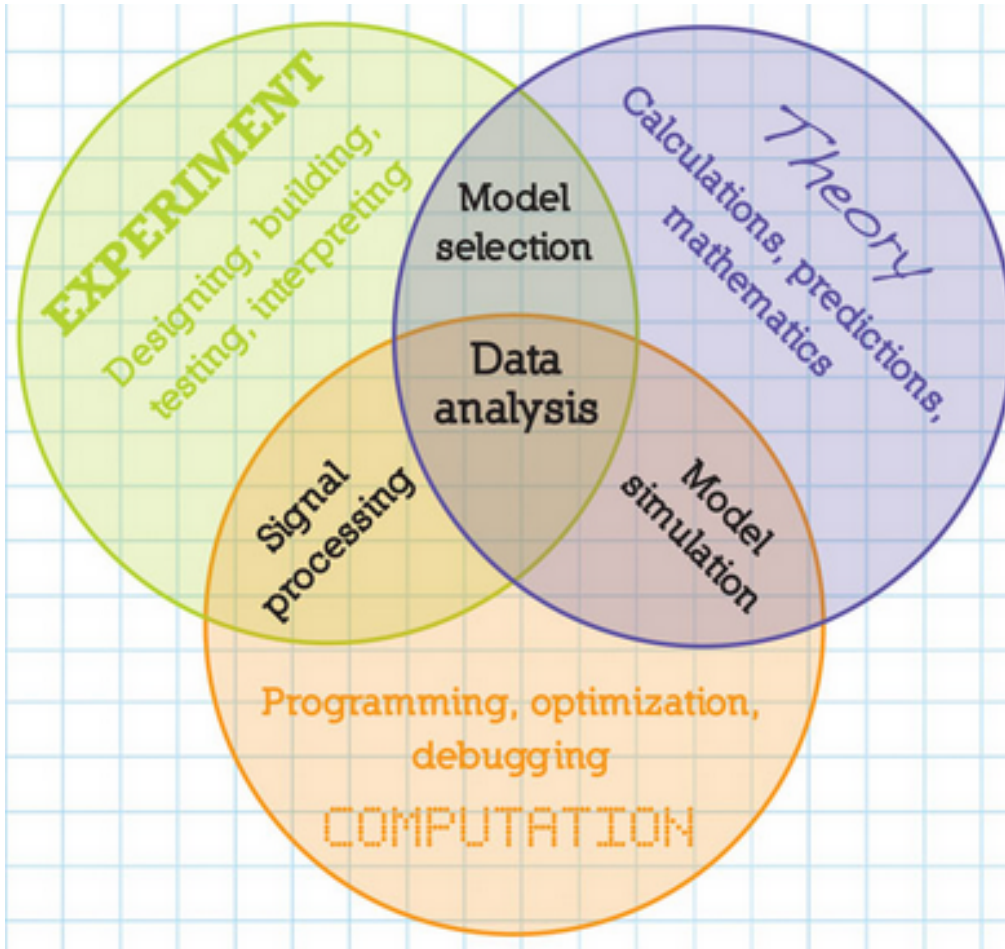
- Strongly correlated electron system
- High spin polarization
- 2-dimensional electron gas
- Metal-insulator transition
- Interfacial ferromagnetism

Wide application range:

Electronics, Spintronics (spin current in magnetic devices), Photonics, Optoelectronics, Photovoltaics...

Power conversion efficiency ~ 22% (2017)





Density functional theory (DFT)

- Computational quantum mechanical modelling
- Compute the electronic structure of matter
- Ground state properties of a system

⇒ Electron density

$$n(\mathbf{r}) = \sum_i \psi_i^*(\mathbf{r}) \psi_i(\mathbf{r})$$

⇒ Functionals:

Functions of another functions

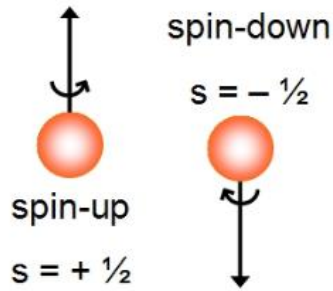
Exchange interactions, magnetic moments, magnetic ground states...

⇒ Excited state properties (DFPT)

⇒ Time-dependent DFT (TDDFT)

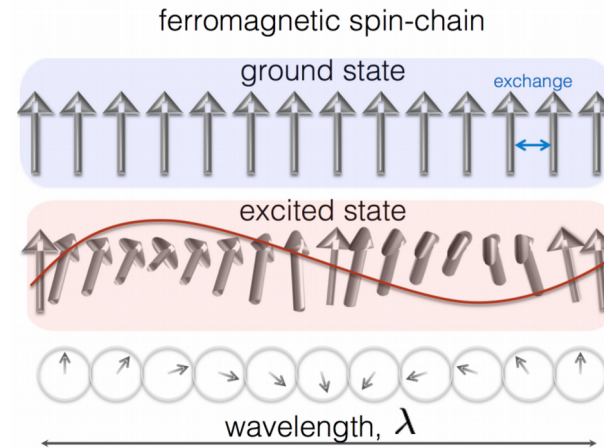
(Quantum Espresso, VASP, Wien2K...)

Spin: an intrinsic angular momentum of the electron

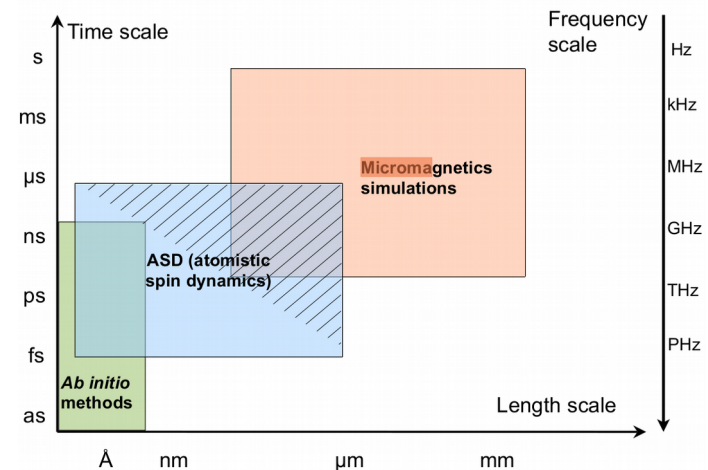
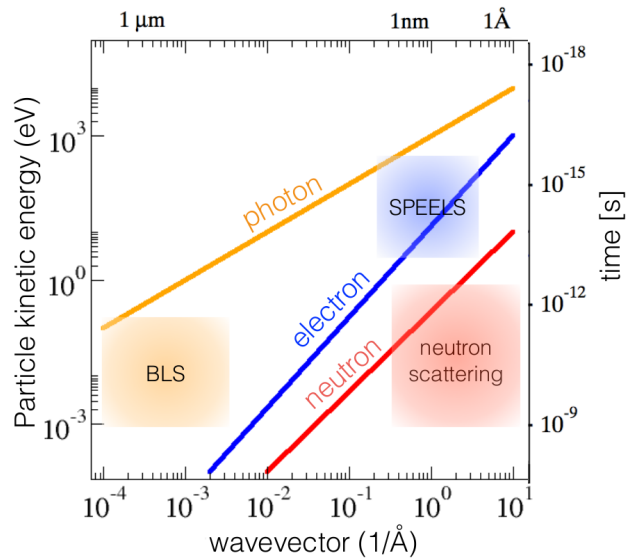


The two possible spin polarisations of the electron

http://cronodon.com/Atomic/quantum_angular_momentum.html



Springer Verlag (2005)



Experimental techniques:

neutrons, electrons, photons scattering experiment

Theoretical methods:

Ab initio calculations:(DFT,time-dependent DFT, Frozen magnon approach...)

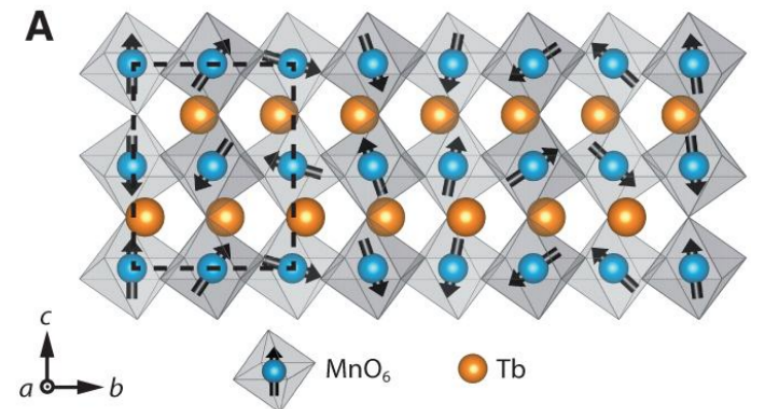
Atomistic spin dynamics;

Micromagnetics simulations;

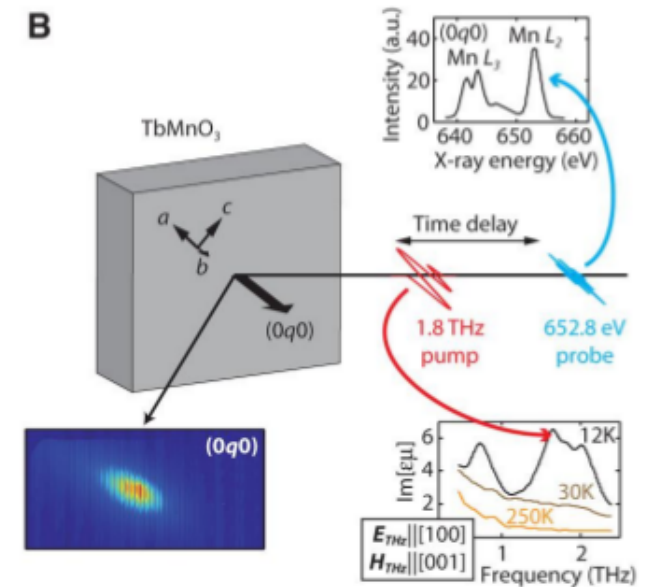
Experimental findings

Large-amplitude spin dynamics driven by a THz pulse in resonance with an electromagnon^[1]

- Time-resolved resonant soft x-ray diffraction
- Intense THz pulses (1.8)
- Using electric field of light on a sub picosecond time scale
- Control the spin dynamics of the multiferroic TbMnO_3



Magnetic structure of TbMnO_3

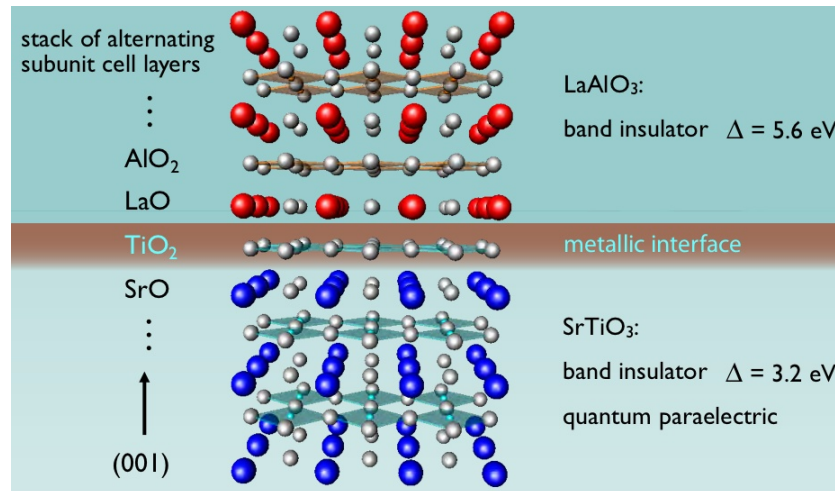


Schematic of the experiment

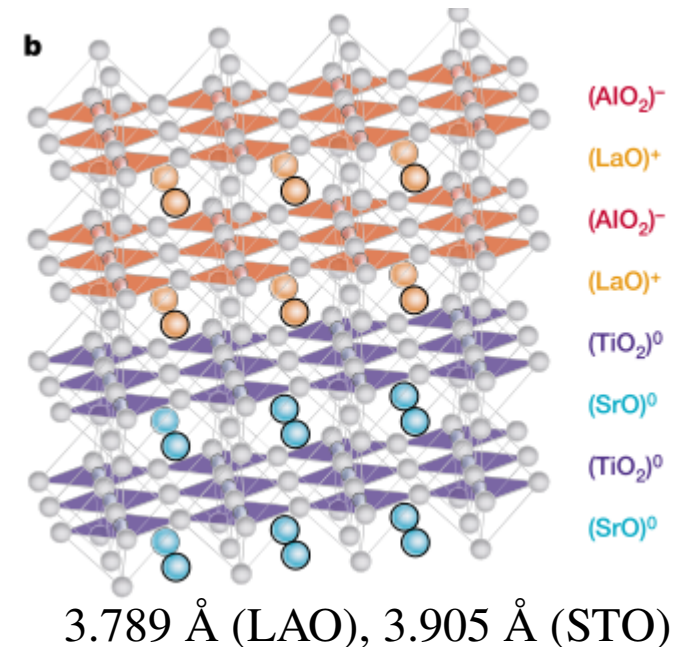
[1] T. Kubacka, *Science*, **343**, 1333, 2014

LaAlO₃/SrTiO₃ heterointerface

A high-mobility electron gas at the LaAlO₃/SrTiO₃ heterointerface^[2]



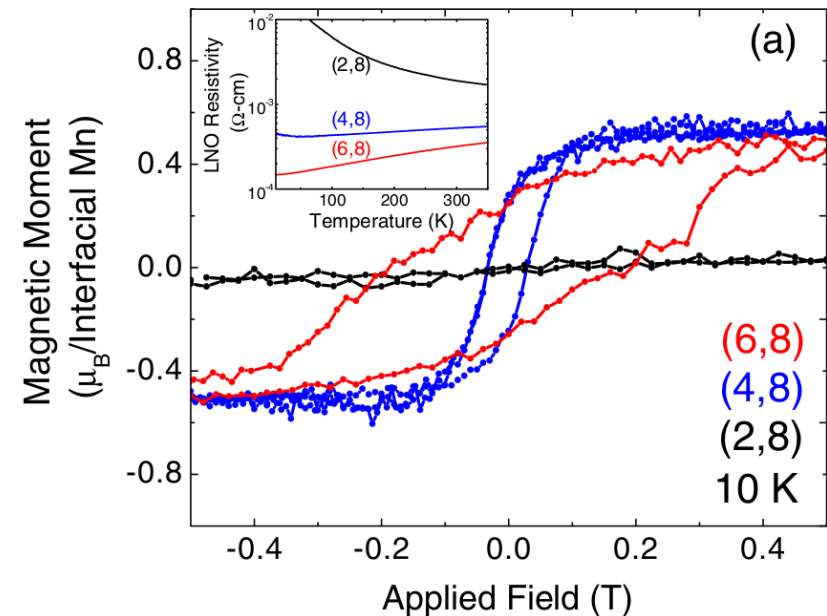
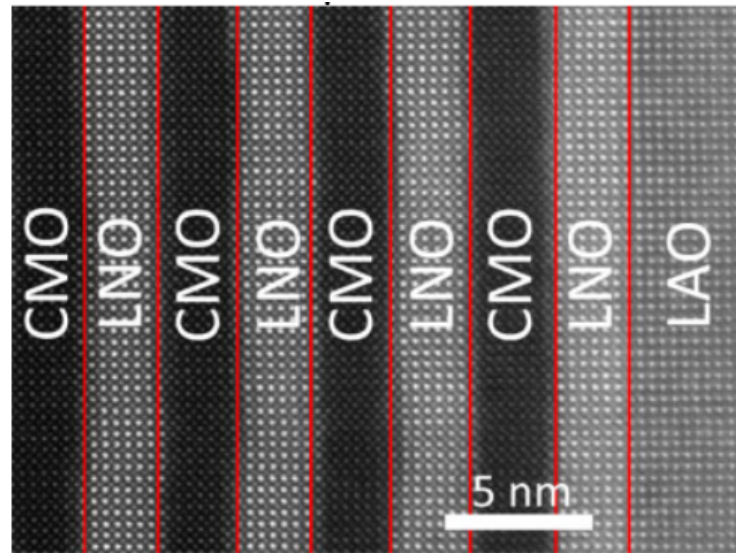
<https://www.slideshare.net/nirupam12/charge-spin-and-orbitals-in-oxides>



- Pulsed laser deposition
- Polarity discontinuity
- Hole-doped interface (SrO)⁰/(AlO₂)⁻ is insulating
- Electron-doped interface (LaO)⁺/(TiO₂)⁰ is conducting
- High-mobility electron gas >10000cm²/v.s

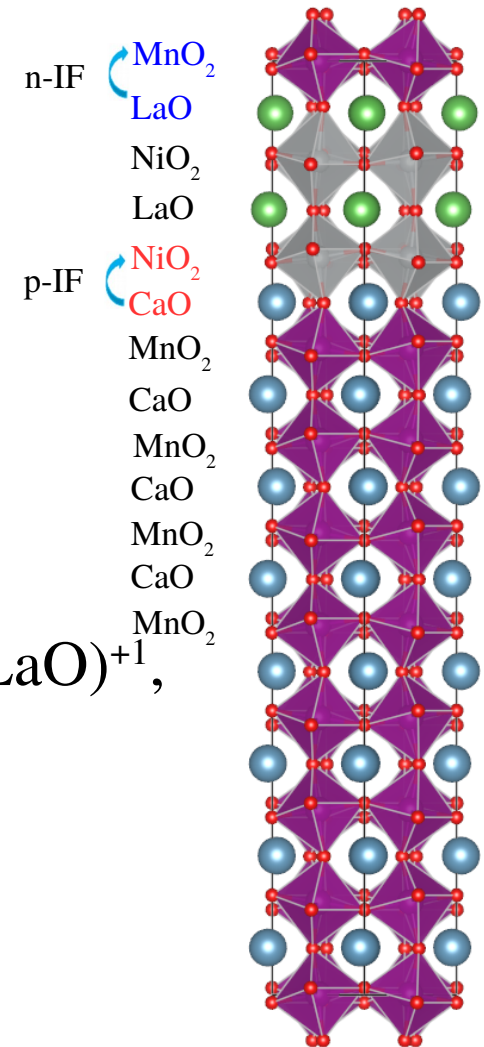
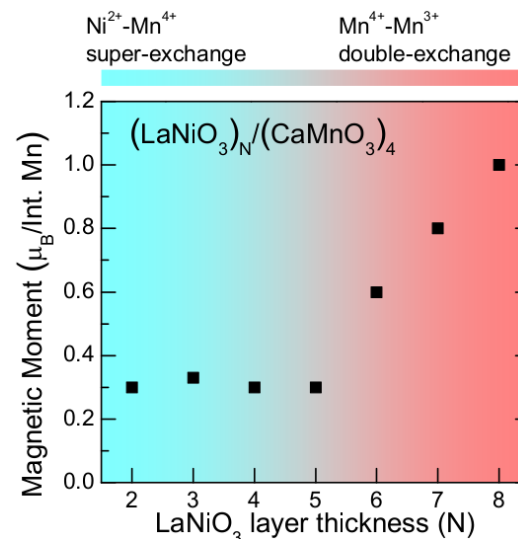
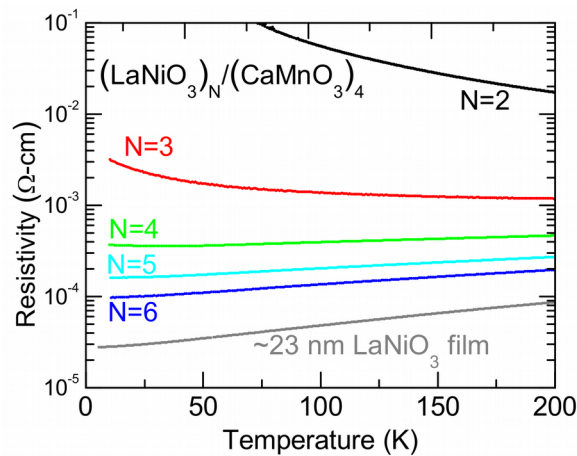
[2] A. Ohtomo et al, Nature **427**, 423, 2004

Interfacial Ferromagnetism in LaNiO₃/CaMnO₃ Superlattices^[3]



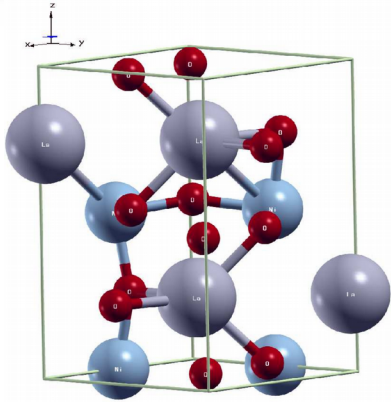
- Pulsed laser deposition
- CaMnO₃: AFM insulator, LaNiO₃: paramagnetic metal
- Thickness dependent metal-insulator transition
- Ferromagnetism at interface

Role of polar compensation in interfacial ferromagnetism of $\text{LaNiO}_3/\text{CaMnO}_3$ superlattices^[4]

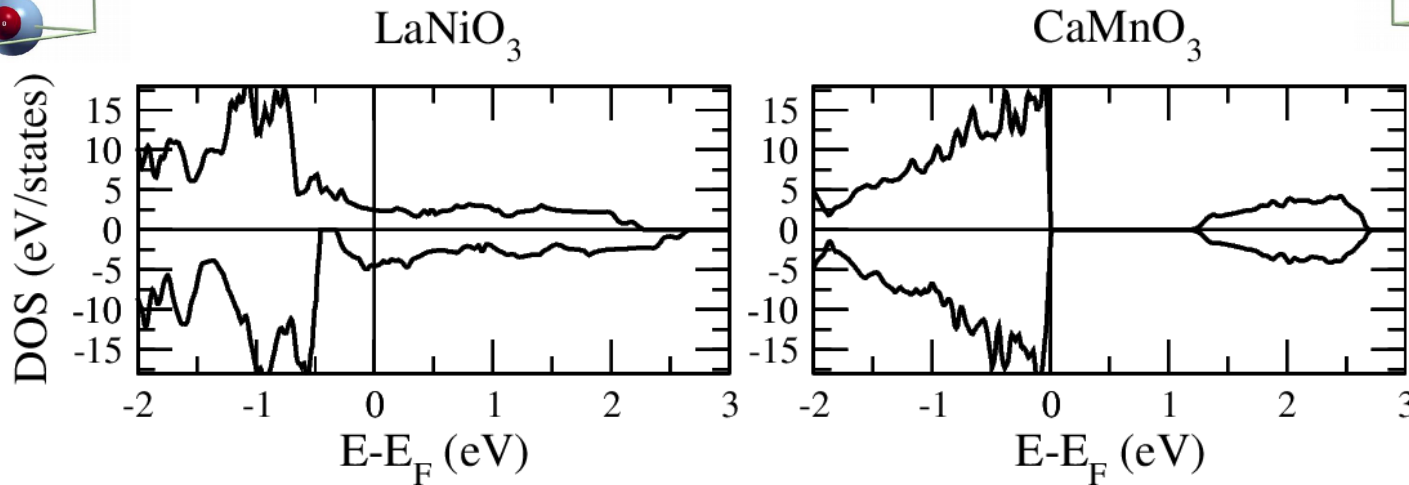
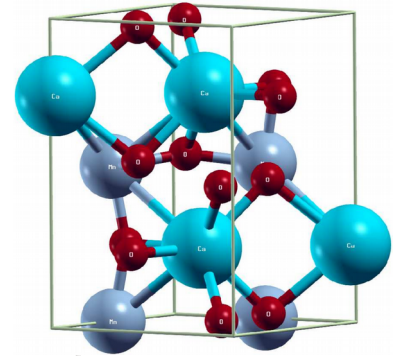


- Polar compensation due to polar mismatch: $(\text{MnO}_2)^0$, $(\text{LaO})^{+1}$, $(\text{CaO})^0$, $(\text{NiO}_2)^{-1}$
- Magnetic exchange interaction: spin flip process
- Ferromagnetic signal for all superlattices
- Ni magnetism

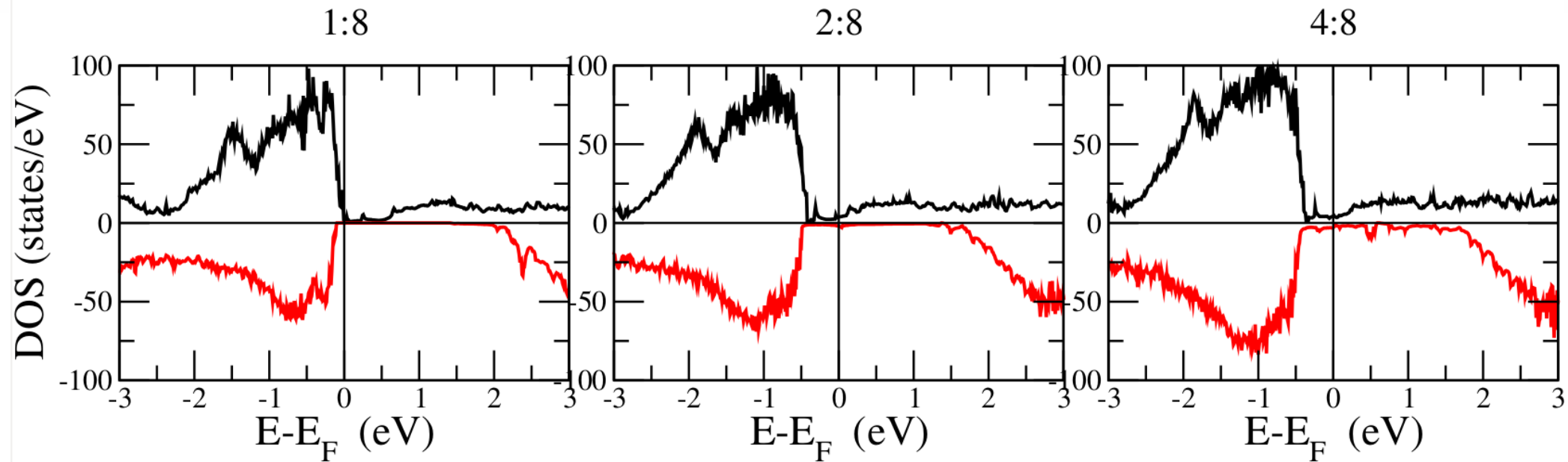
LaNiO₃, CaMnO₃ bulk (DFT)



LaNiO₃ : Paramagnetic metal
 CaMnO₃ : Antiferromagnetic insulator

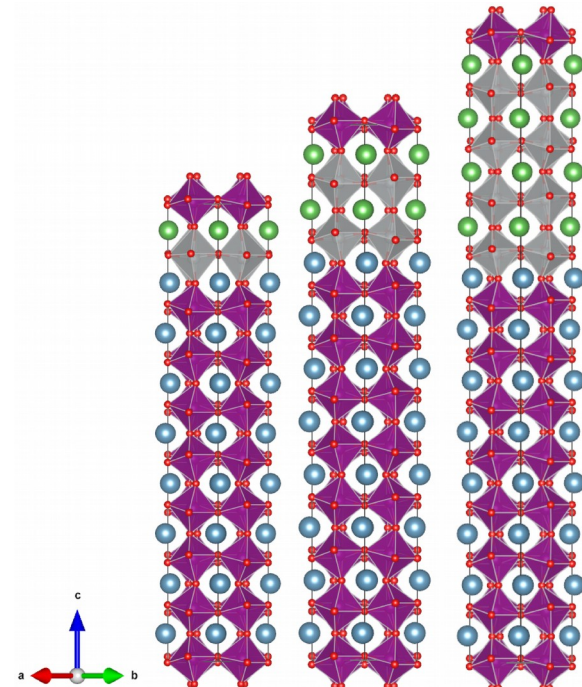


- Coulomb interaction term U : correlated nature of the localized d-orbitals
- Ferromagnetism is favorable when $U > 0$ eV for LaNiO₃
- Antiferromagnetism is favorable $U \leq 3$ eV for CaMnO₃
- Bulk electronic structure is well reproduced

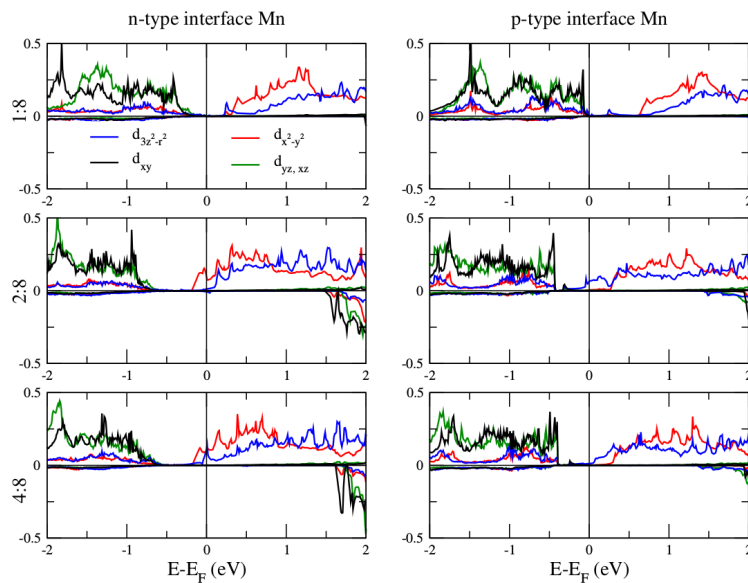
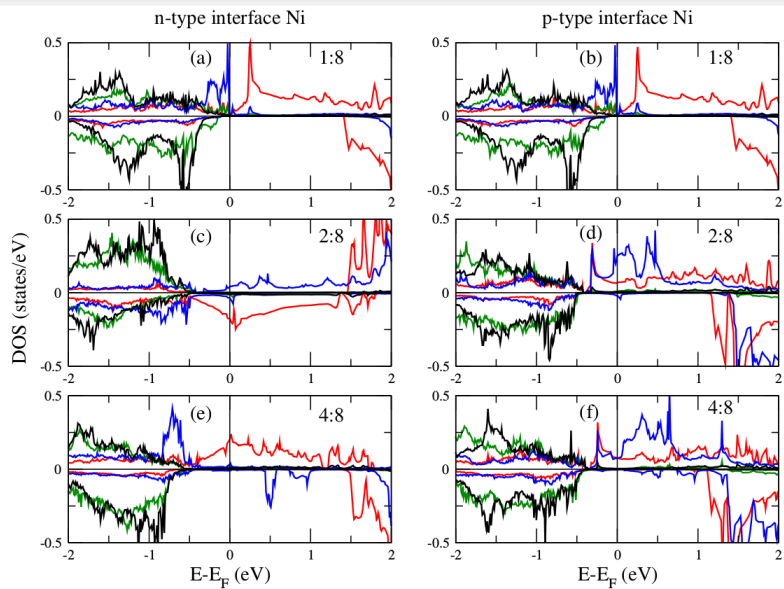


- O-Mn-O off-centering along z axis toward p-IF up by up to 0.05 Å
- More tilted MnO₆ octahedra than NiO₆ octahedra
- Orthorhombic ($a^-a^-c^+$) tilt pattern^[5]
- Insulator to metallic phase transition
- Charge transfer and polar discontinuity

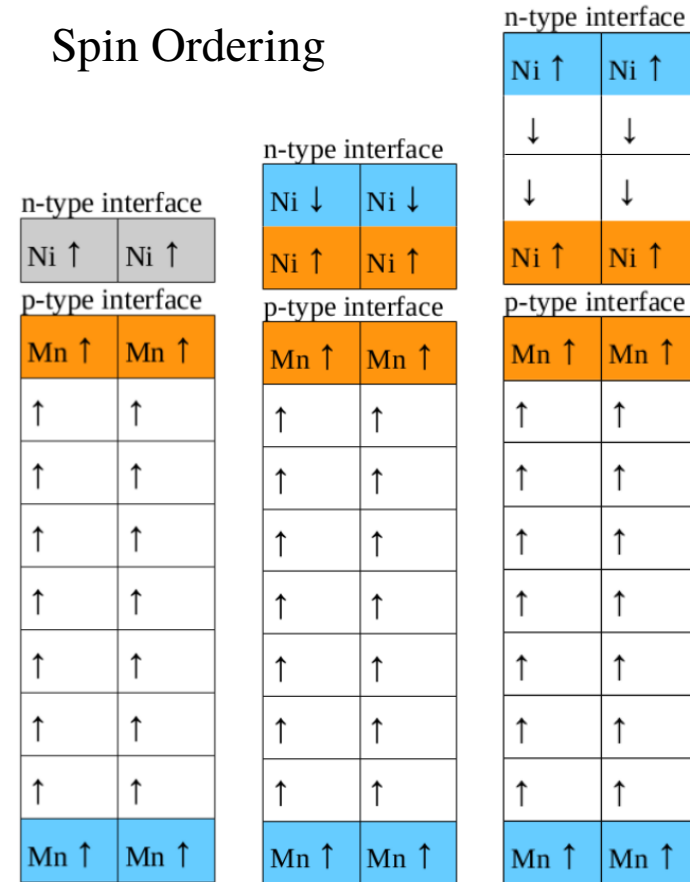
[5] Glazer, A. M. Acta Cryst. B **28**, 3384 (1972)



LaNiO₃/CaMnO₃ superlattice



Spin Ordering



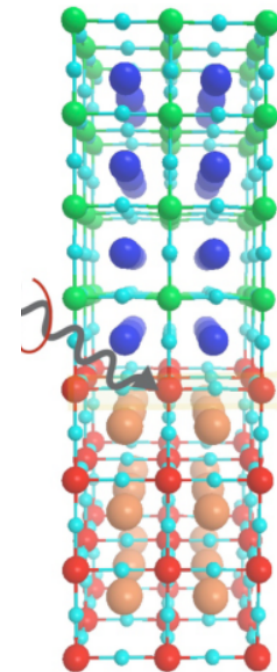
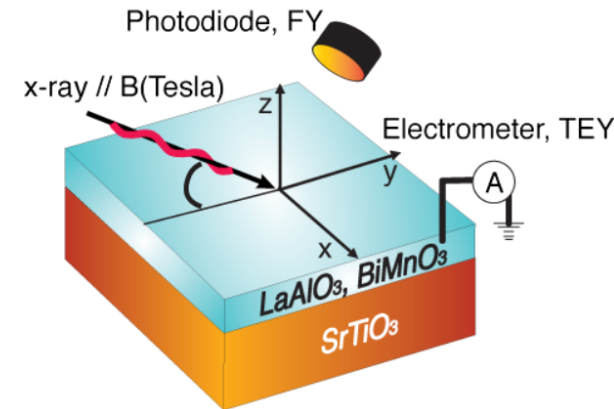
- Charge transfer from LaNiO₃ to CaMnO₃
- Spin exchange in LaNiO₃ layers: AFM ordering
- Magnetic moments: Ni: 0.81~1.19 u_B ; Mn: 3.02~3.07 u_B
- Interplay between exchange interactions due to mixed valence states at interface

BiMnO₃/SrTiO₃ Heterointerface

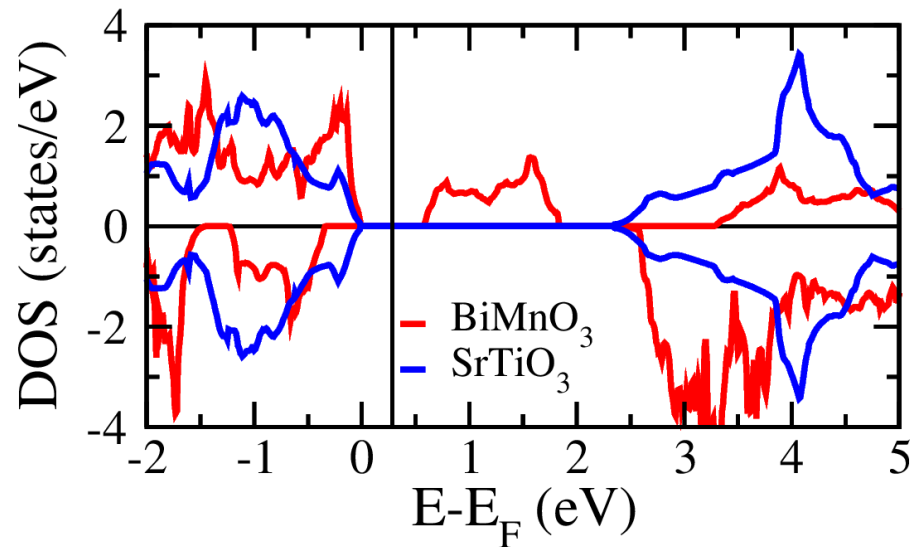
(another interesting candidate)

Origin of Interface Magnetism in BiMnO₃/SrTiO₃ and LaAlO₃/SrTiO₃ Heterostructures^[6]

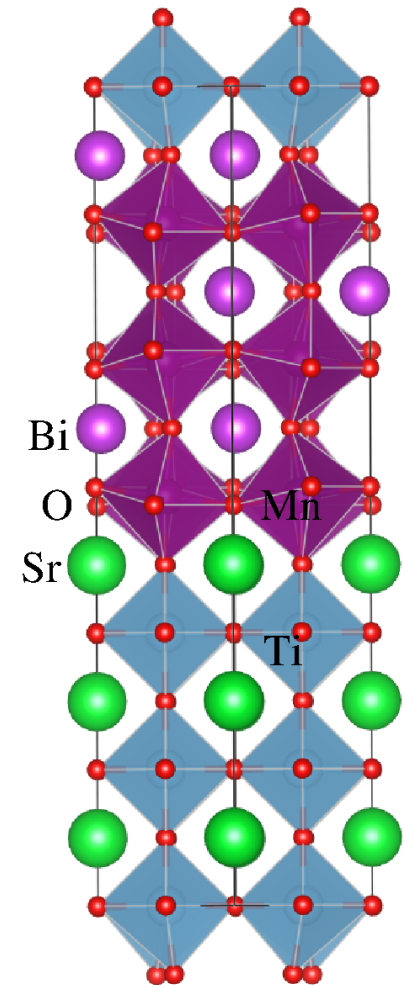
- LaAlO₃, BiMnO₃, SrTiO₃ - non-magnetic insulators
- Interfacial magnetism at both systems
- O vacancy induced magnetism
- Exchange interaction between interface states and localized moments of Mn³⁺



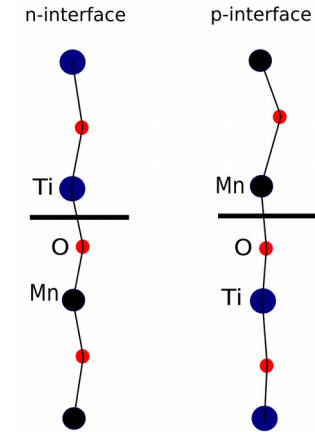
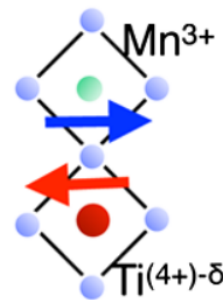
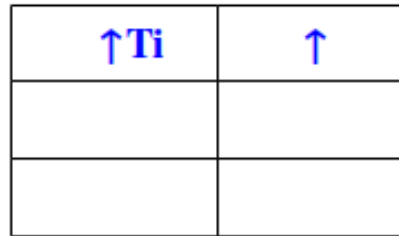
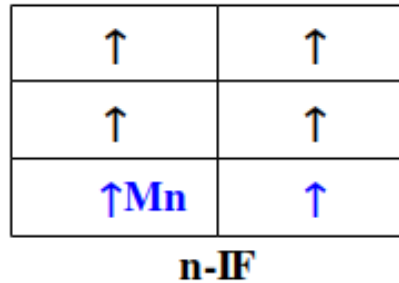
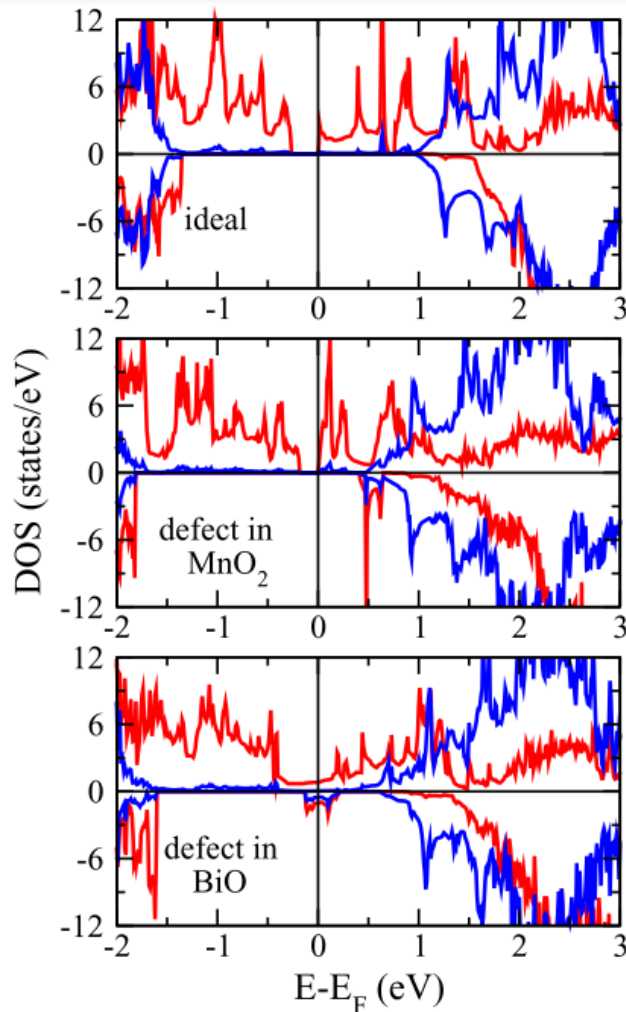
[6] M. Salluzzo, Phys Rev Lett. **111**,087204, 2013



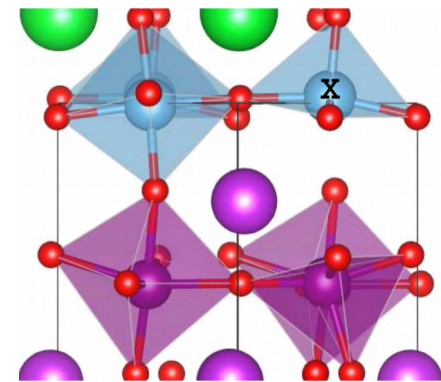
- ▶ SrTiO_3 : Cubic perovskite, non-magnetic insulator
- ▶ BiMnO_3 : Highly distorted, ferromagnetic insulator
- ▶ BiMnO_3 : Low temperature monoclinic phase
- ▶ Small BiMnO_3 band gap
- ▶ Mn magnetic moments: $3.8u_B$
- ▶ Ferromagnetic VS Antiferromagnetic



BiMnO₃/SrTiO₃ superlattice



Distorted SrTiO₃



- ▶ Different behavior of two spin channels
- ▶ Sharp DOS near the Fermi level indicates promising thermoelectricity
- ▶ O vacancy at different layers, spin flip when O vac at BiO layer
- ▶ Strong hybridization of Mn and Ti

Thermoelectricity

Thermoelectricity: direct conversion of heat into electricity or vice versa

Seebeck coefficient electrical conductivity

Figure of merit → $ZT = \frac{S^2 \sigma T}{\kappa}$ thermal conductivity

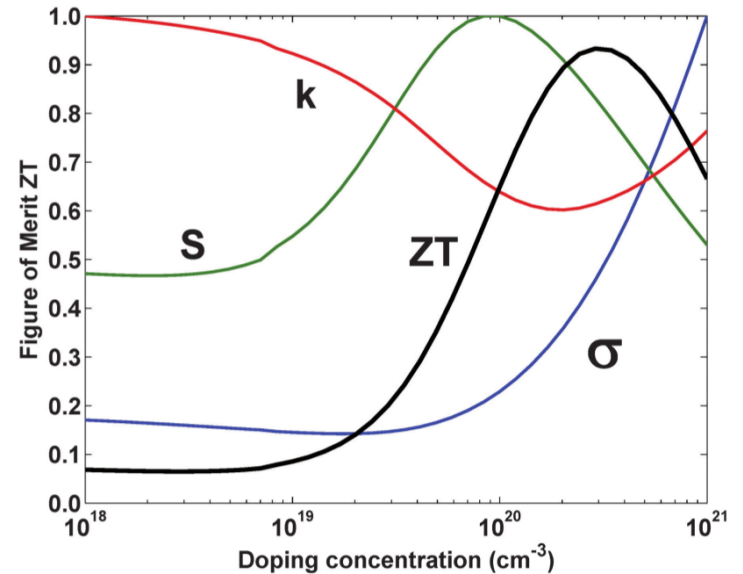
what makes a good thermoelectric → $\uparrow ZT \text{ --- } \uparrow S, \uparrow \sigma, \downarrow \kappa$

Optimal Doping, nanostructuring, spin injection, heterostructure formation...

ZT: $\ll 1$ usually,

Goal : stable material with high ZT

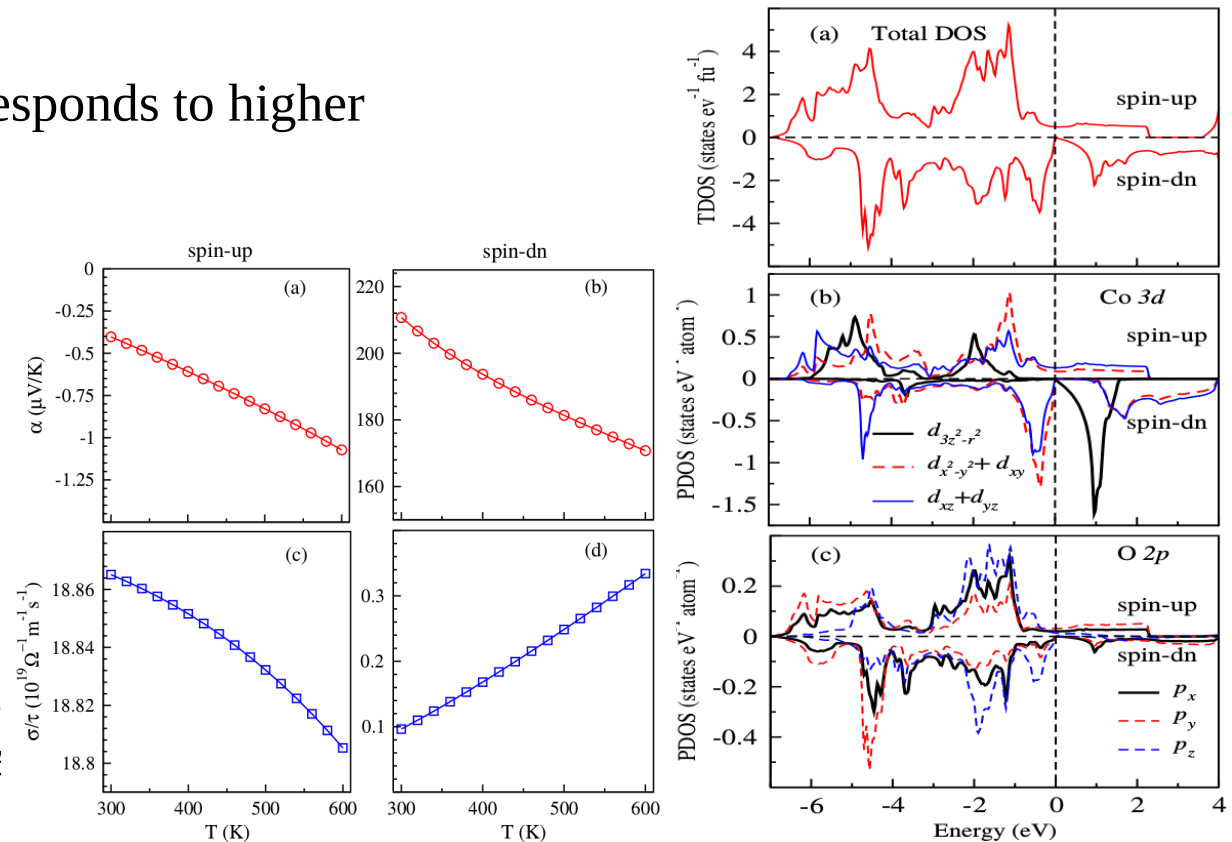
Spin-dependent TE properties—higher ZT



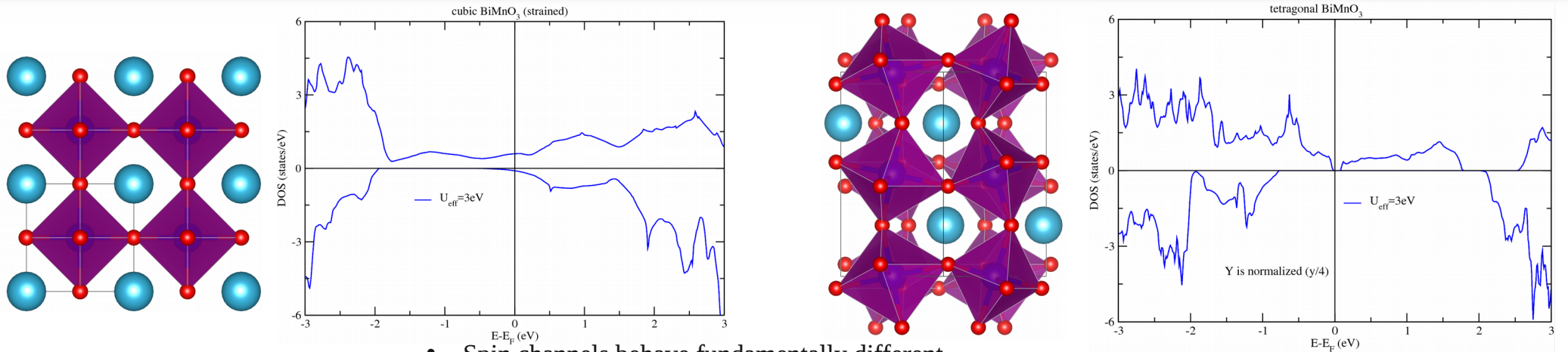
Thermoelectric properties and ZT versus doping concentration at 300 K for n-type Si₈₀Ge₂₀

Effect of two spin channels

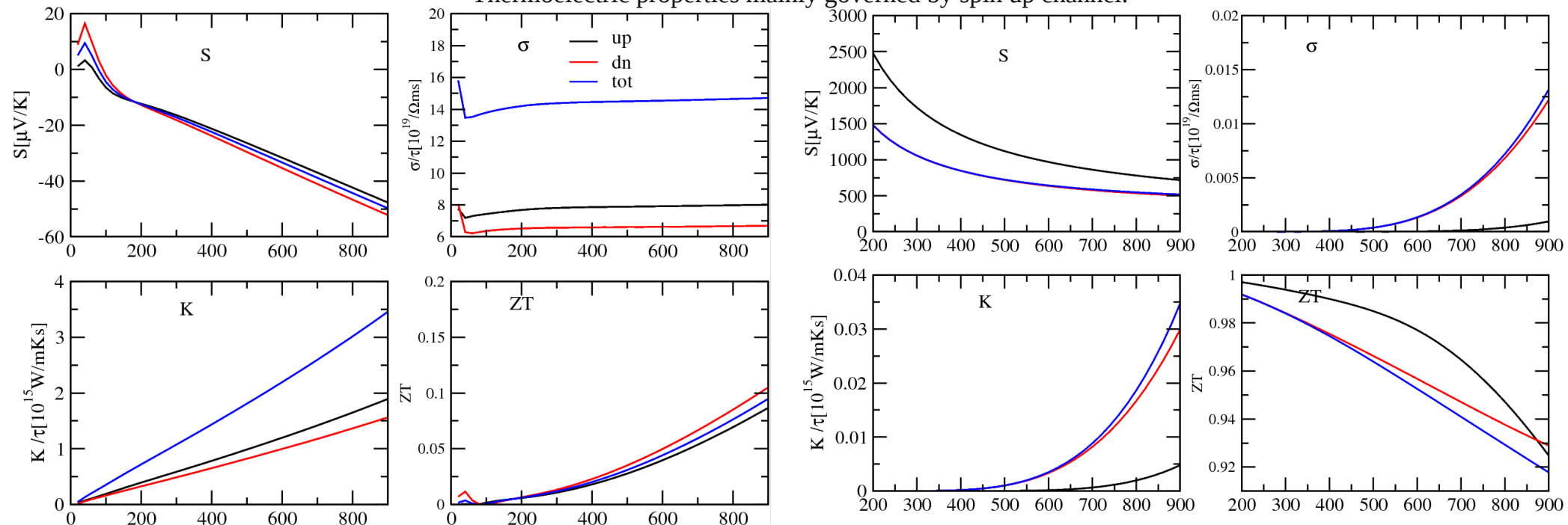
- The contributions in DOS from different orbitals from spin-up and spin-dn channel are different, so different transport behavior is also expected from both the channels.
- Metallic state for one channel corresponds to higher electrical conductivity.
- Semiconducting state corresponds to lower electrical conductivity.
- Thermal excitation of spin moments can alter the magnetic state of materials.
- Corresponding transport properties can alter with different spin channels.



BiMnO₃ lattice distortion and TE figures

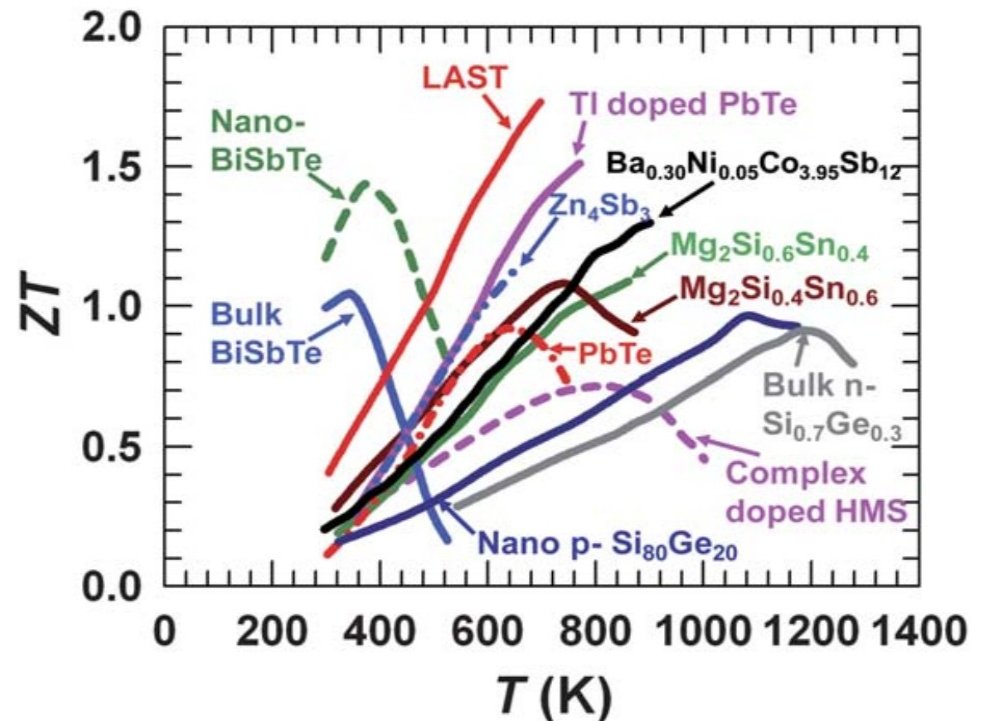


- Spin channels behave fundamentally different.
- Thermoelectric properties mainly governed by spin up channel.



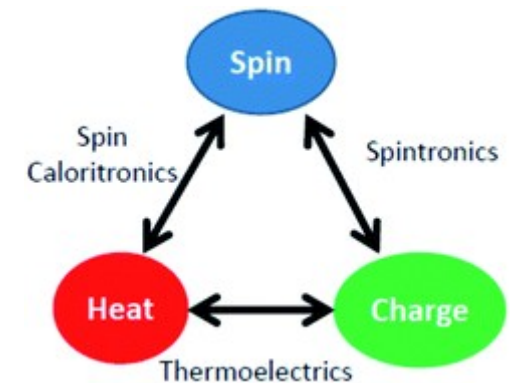
- Reasonable performance when compared to existing ‘good thermoelectrics’.
- Ferromagnetic spin exchange plays dominant roles in these perovskite IFs.

- Figure of merit of approximately 1.5 (600 K) can be achieved in current 'good thermoelectric' systems
- $\text{BiMnO}_3/\text{SrTiO}_3 \sim 1$ (200-400 K)
- With modification in induced spin channels, perovskite IF can be very efficient 'thermoelectric material'
- Spin exchange and dynamics play important role
- Thermoelectric materials based on perovskite oxides, spin caloritronics



J. Mater. Chem. **21**, 4037 (2013)

- Perovskite materials are good candidates for electronic structural, spin transport and dynamical application
- The interfacial magnetism and metal-insulator transition were achieved in $\text{LaNiO}_3/\text{CaMnO}_3$; Role of spin dynamics
- Good thermoelectric property of BiMnO_3 , tunability via different spin channels, doping concentration.
- Manipulation of TE of superlattice via strain, defect engineering
- Spin dependent heat transport, spin caloritronics.



Thank you



Investigate: Excited states, optical, charge, spin dynam

Package: Octopus, MD, Qprob etc

<https://www.sciencedirect.com/science/article/pii/S03759601163693>

It has been shown also that a spin current can be induced by heating with ultrafast laser pulses [101], [102].

heat-driven spin currents

BoltzTraP code is based on the Semi-classical Boltzmann transport theory

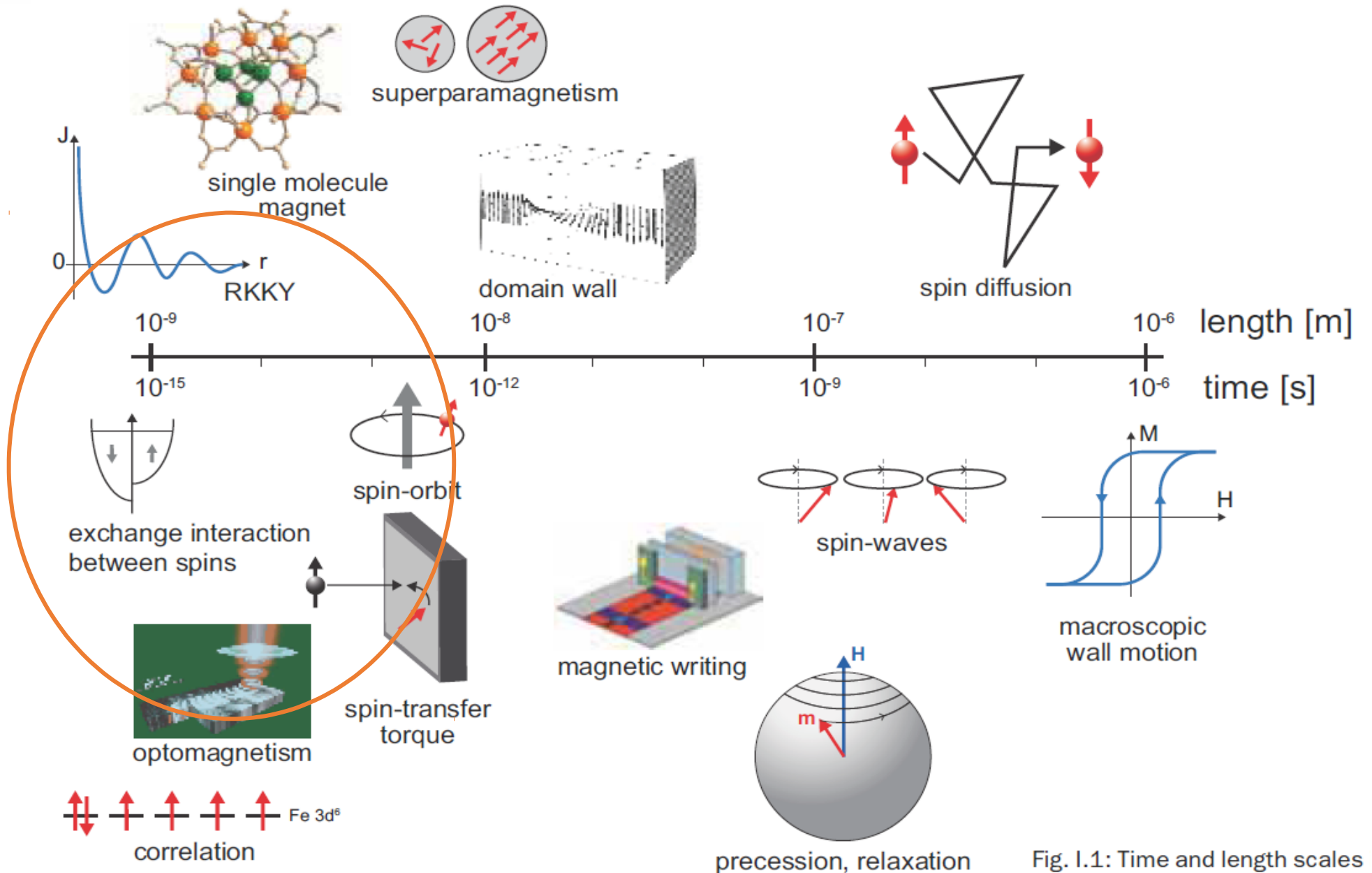
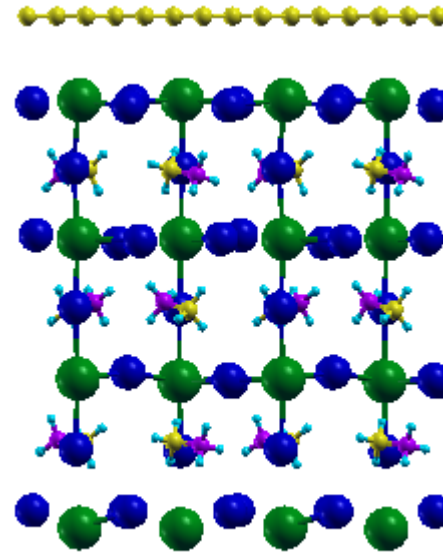
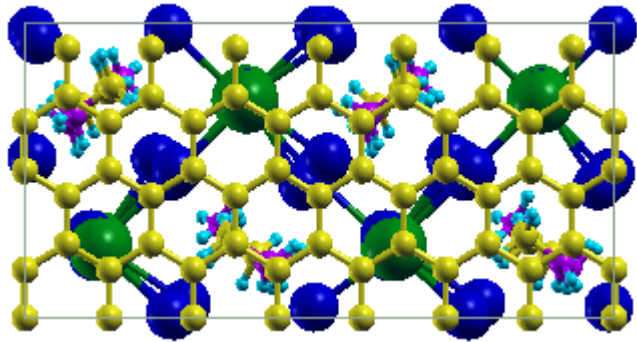


Fig. I.1: Time and length scales

Future Plan

Hybrid Perovskites with 2D materials

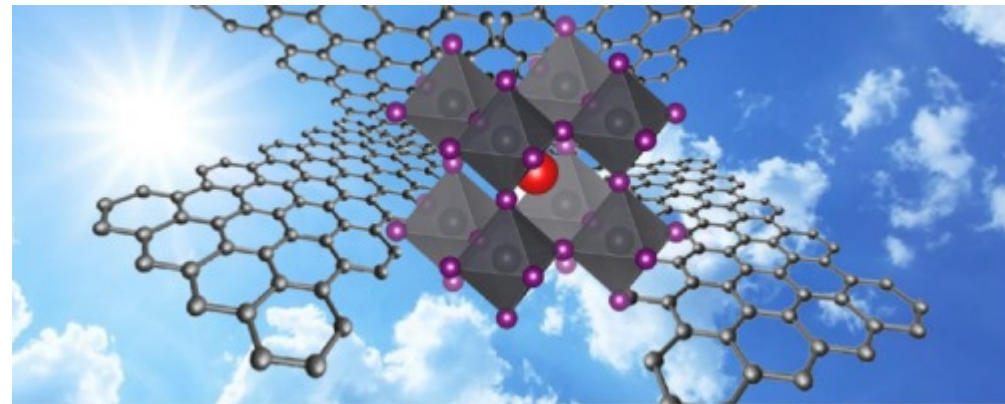


*Photo-induced electron–hole pairs in the pristine perovskite recombine within a few picoseconds^[1].

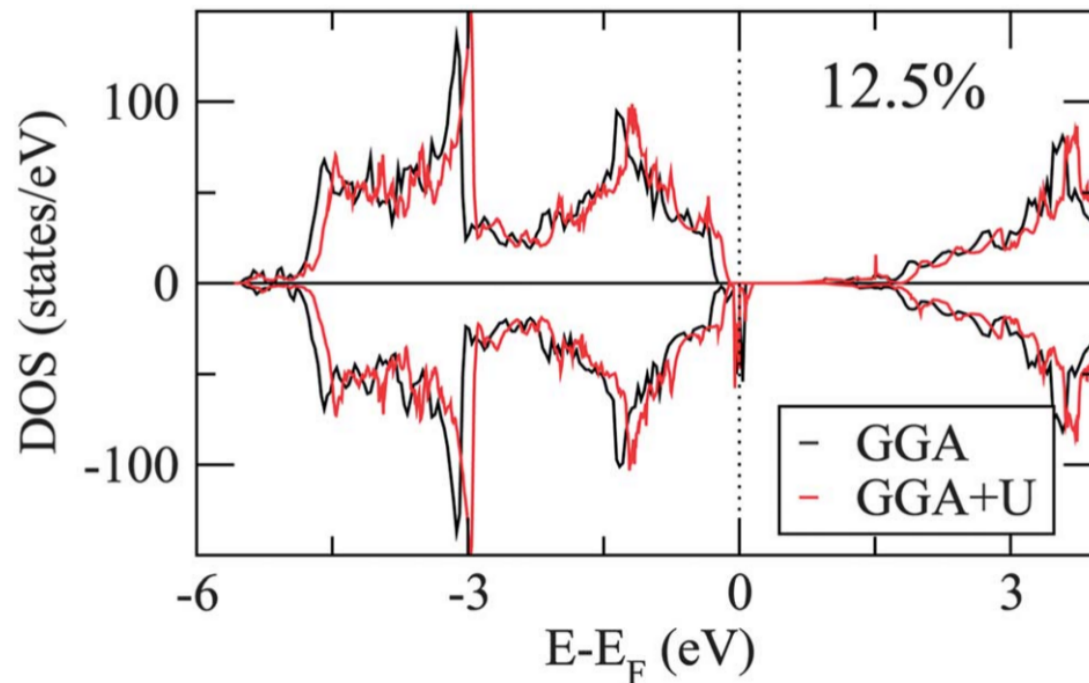
*Photoelectronic applications

*Optoelectronic applications

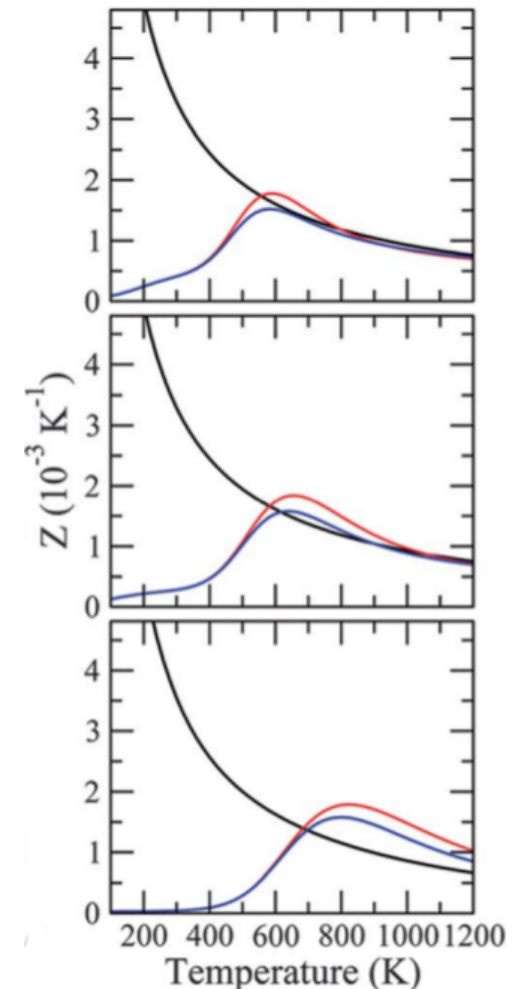
[1] Adv. Mater. 27, 41–46 (2015)



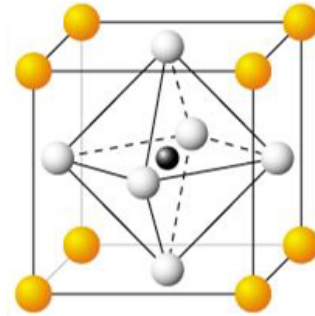
Half-metallic perovskite superlattices with colossal thermoelectric figure of merit^[7]



- ▶ Insulator to a half-metallic transition via Co doping
- ▶ High value of the spin Seebeck coefficient
- ▶ Colossal figure of merit of $0.45 \cdot 10^{-3} \text{K}^{-1}$
- ▶ Spin-caloritronics



CaTiO₃ oxide mineral, 1839, Russia



A: Rare-earth or alkali-metal cation
B: 3d, 4d, 5d transition metal cations

ABO₃ perovskite structure

bulk ABO₃, layered perovskites, double perovskite, thin films, superlattices, organo-halide perovskites...

Manganites: LaMnO₃, CaMnO₃, BiMnO₃, La_{1-x}Sr_xMnO₃, SrMnO₃ etc

Titantes: SrTiO₃, LaTiO₃, CaTiO₃, BaTiO₃ etc

Ferrites: BiFeO₃, LuFe₂O₄ etc

Nicklates: LaNiO₃ etc

Enhanced photovoltaic performance of perovskite $\text{CH}_3\text{NH}_3\text{PbI}_3$ solar cells with freestanding TiO_2 nanotube array films^[3]

- >90% of light absorption
- Reduced charge recombination rate
- Improved conversion efficiency
- Enhanced photovoltaic performance
- Solar cell device

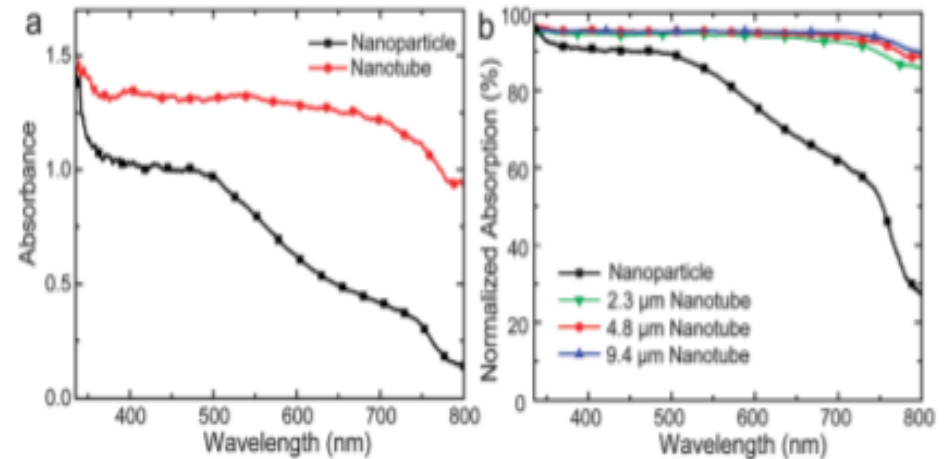
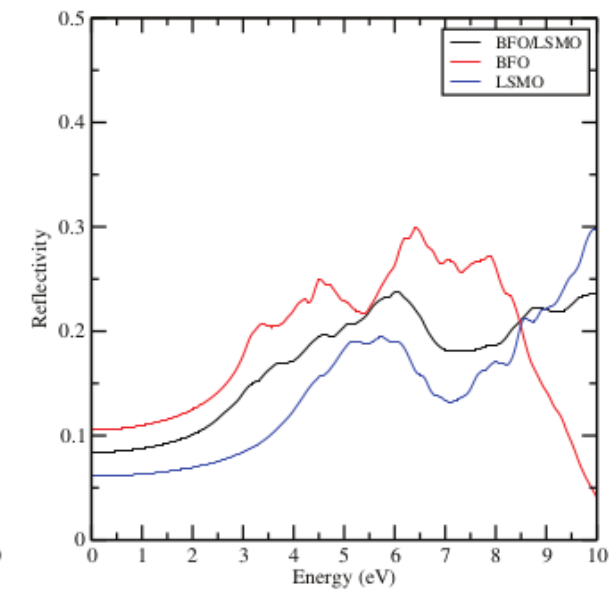
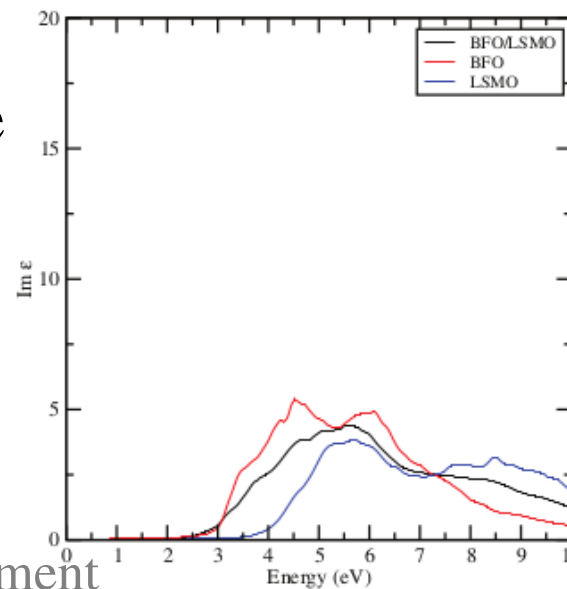
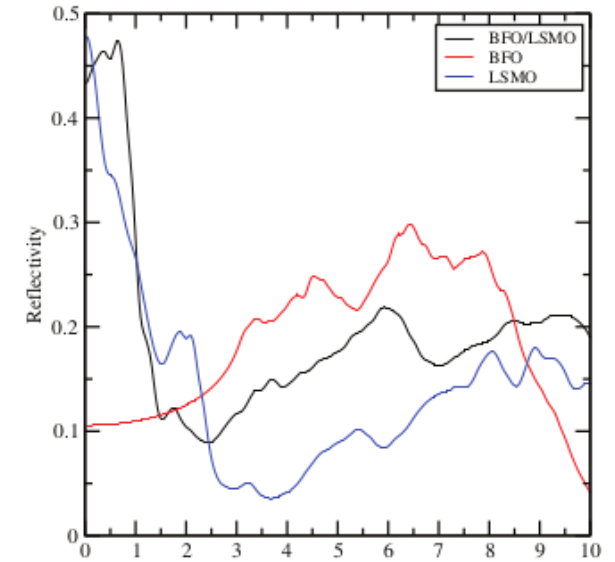
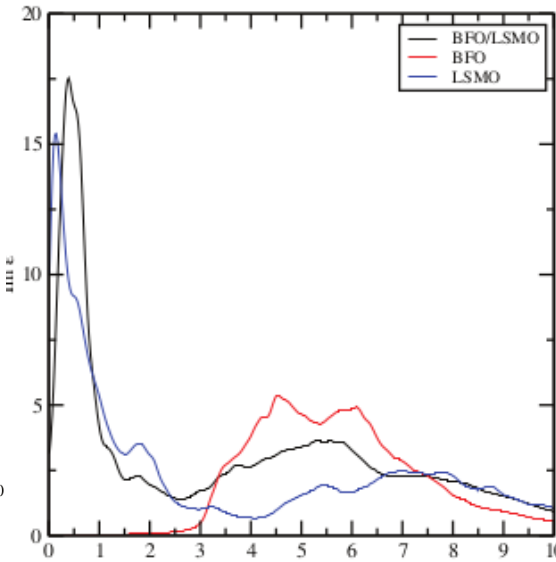
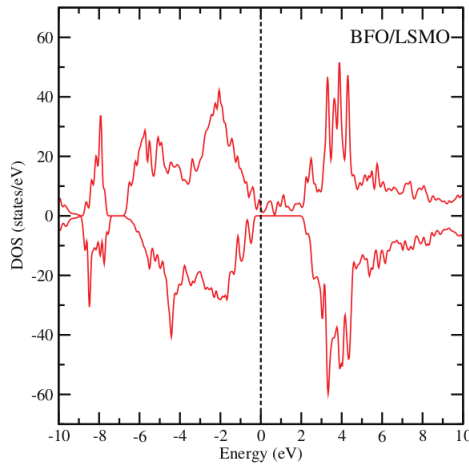
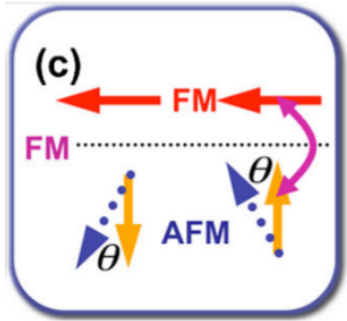


Fig. 3 (a) UV-Vis absorption of $\text{CH}_3\text{NH}_3\text{PbI}_3$ sensitized TiO_2 nanoparticle and TiO_2 nanotube electrode. (b) Normalized adsorption spectra as a function of TiO_2 nanotube thickness compared with TiO_2 nanoparticle electrodes.

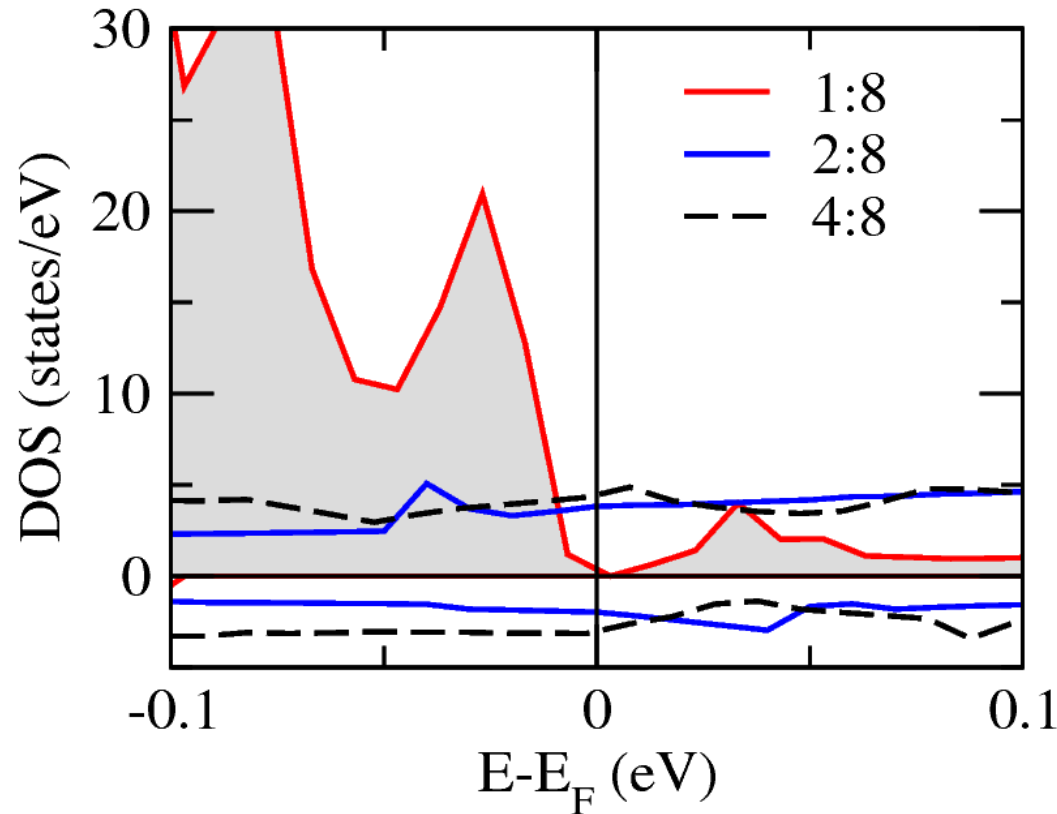
[3]Chem. Commun., 50, 6368, 2014



- Half-metallic character
- Optical properties resemble the DOS
- Combined property
- Spintronics

[6]PRL **105**, 027201 (2010)--experiment

[7]EPL, **102** (2013) 67009--DFT



Ising model: In order to map out the energetic interactions between the magnetic and rotational degrees of freedom, we utilize a modified Ising model. The Ising Model was originally developed to study properties of interacting lattice systems, such as ferromagnetic materials.¹⁹ In the model, an arbitrary lattice of N sites is set up. A given site can be filled with a particle with some relevant property specified, such as spin, and is assigned an occupation term σ_i , where $\sigma_i = 0$ if site i is empty, and $\sigma_i = 1$ if site i is occupied. The energy contribution due to the presence of a particle in site i is designated as the field term, h_i . Energy contributions due to particle interactions in neighboring sites are captured by the nearest-neighbor interaction term J_{ij} , where i and j are two distinct sites. These nearest-neighbor interactions can be attractive or repulsive. Further interactions can also be accounted for, such as next-nearest-neighbor interactions. These would be assigned a different set of interaction terms $J_{j,k}$. The total energy of the N -site lattice is then calculated as:

The Ising Model allows derivation of a reduced-order Hamiltonian for the system under consideration. Simulated formation enthalpies are used to calculate relevant Ising Model coefficients for the system. Through the use of coefficients derived with the Ising Model, the new Hamiltonian can be implemented in a Monte Carlo simulation of larger bulk structures. These simulations introduce and allow the quantification of the effect of thermal disorder on the system. Coefficients derived from the Ising Model were then used to simulate larger bulk cells with higher degree of